

Critical dynamics of decoherence

Bogdan Damski, H. T. Quan, and Wojciech H. Zurek

Theoretical Division, MS B213, Los Alamos National Laboratory, Los Alamos, NM, 87545, USA

We study decoherence induced by a dynamic environment undergoing a quantum phase transition. Environment's susceptibility to perturbations – and, consequently, efficiency of decoherence – is amplified near a critical point. Over and above this near-critical susceptibility increase, we show that decoherence is dramatically enhanced by non-equilibrium critical dynamics of the environment. We derive a simple expression relating decoherence to the universal critical exponents exhibiting deep connections with the theory of topological defect creation in non-equilibrium phase transitions.

PACS numbers: 03.65.Yz, 05.30.Rt

I. INTRODUCTION

Decoherence of a qubit coupled to an environment is studied with the central spin models. In addition to being a workhorse for understanding of quantum to classical transition [1–3], central spin models describe loss of qubit's coherence in NV centers in diamond [4], quantum dots in semiconductors [5], NMR experiments [6, 7], etc. The environment, usually regarded as a destroyer of quantum coherence and entanglement, has been recently proposed to enhance sensitivity of a magnetometer based on the central spin system [8]. Therefore, understanding how the environment influences qubit's state is central to quantum computing and metrology.

So far, studies of decoherence focused mainly on systems prepared in Schrödinger cat-like superpositions instantaneously coupled to an otherwise static environment described by time-independent Hamiltonian. We consider instead a spin-1/2 system coupled to a driven environment. The environment undergoes a quantum phase transition (QPT) as it is driven through the quantum critical point by the change of the external field (e.g., a magnetic field in the Ising chain depicted in Fig. 1). Decoherence occurs because the environment “monitors” the system and “finds out” its pointer states (i.e., effectively classical states preserved in spite of decoherence [1–3]). This means that each pointer state remains untouched, but makes a distinct imprint on the quantum state of the environment. How close to orthogonal are these record states determines how well the environment knows about the system. Their overlap is the decoherence factor $d(t)$ multiplying off-diagonal terms of the reduced density matrix of the qubit.

Effectiveness of decoherence depends on how easy it is to perturb – “write on” – the environment: Its “stiffness” is determined by its Hamiltonian as well as by its state. For the Ising environment, Hamiltonian-induced stiffness is due to either spin-spin interactions or the external field (Fig. 1). When the two balance, the environment is at the critical point, where it is most susceptible to perturbations. Decoherence is expected to be strongest there. This was already seen in *static* critical environments [9, 10]. In our system the environment is *not* static: It is driven across the phase transition, so

its instantaneous state – and thus decoherence – is determined by both its Hamiltonian and its history. We show that the latter profoundly affects qubit's decoherence rate.

The aim of this paper is to understand how a driven critical environment affects decoherence of a qubit. For clarity of our discussion, which can be extended to more complicated systems, we consider an exactly solvable paradigmatic model of a QPT: the Ising chain coupled to a central spin-1/2 (Fig. 1). We show analytically that decoherence is enhanced by the nonequilibrium transition and exhibit interesting dynamics characterized by the transition rate, coupling strengths and ground state fidelity. We also show that the time-dependent decoherence factor encodes both universal properties of the system associated with quantum criticality (critical exponents) and rich system-dependent (non-universal) features. Our work combines theory of decoherence with rapidly growing fields of dynamics of QPTs [11–16] and quantum information [17–20]. In the latter context, our study can be regarded as a dynamic generalization of the so-called fidelity approach to QPTs [17, 18]. We would also like to mention that in the context of dynamics of QPTs decoherence has been studied in [21–23].

II. BASICS OF QUENCH DYNAMICS

To study non-equilibrium environment – qubit evolution we characterize dynamics of an environment driven across a critical point. This is done using the quantum version [11–13] of the Kibble-Zurek (KZ) theory [24, 25]. The environment is quenched by decreasing the external field

$$g(t) = g_c - t/\tau_Q, \quad (1)$$

where g_c stands for strength of the external field at the critical point, the quench time τ_Q is inversely proportional to the quench speed, and time t goes from $-\infty$ to $+\infty$. A QPT is characterized by vanishing excitation gap $\Delta_0|g - g_c|^{z\nu}$ and divergent correlation length $\xi_0/|g - g_c|^\nu$, where z and ν are the critical exponents, while Δ_0 and ξ_0 are constants [26]. There are two relevant time scales during a quench: the system reaction

time given by $\hbar/\Delta_0|g-g_c|^{z\nu}$ and the time scale of change of the Hamiltonian given by $(g(t) - g_c)/\frac{d}{dt}(g(t) - g_c)$. Away from the critical point the reaction time is short compared to quench time scale and so evolution is adiabatic. Near the critical point opposite happens and evolution is approximately diabatic. The border between the two regimes lies at a distance \hat{g} from the critical point. Equating the two timescales, we get

$$\hat{g} \sim \tau_Q^{-1/(1+z\nu)}. \quad (2)$$

KZ theory also predicts that there is a non-equilibrium length scale $\hat{\xi}$ imprinted onto the post-transition state of the system [25]. It is given by the coherence length at the border between adiabatic and impulse regimes where the state of the many-body system freezes out:

$$\hat{\xi} = \xi(\hat{g}) \sim \tau_Q^{\nu/(1+z\nu)}. \quad (3)$$

This scale yields e.g. a typical distance between topological defects created during a symmetry-breaking QPT. It also suggests that non-equilibrium excitations resulting from the quench should encode a characteristic momentum scale

$$\hat{k} \sim \hat{\xi}^{-1} \sim \tau_Q^{-\nu/(1+z\nu)}. \quad (4)$$

III. THE MODEL

We consider decoherence of the qubit coupled to a driven Ising chain undergoing a QPT (Fig 1). The Ising Hamiltonian is

$$\hat{H}_\mathcal{E} = -\sum_{j=1}^N (\sigma_j^x \sigma_{j+1}^x + g(t) \sigma_j^z),$$

while its coupling to the qubit reads

$$\hat{H}_{S\mathcal{E}} = -\delta \sum_{j=1}^N \sigma_j^z \sigma_S^z.$$

Above the environment size $N \gg 1$, the system-environment coupling $\delta \ll 1$, and σ_S^z is the Pauli matrix of the qubit. Ising chain in a transverse field has been experimentally studied in [27, 28]. The coupling $\hat{H}_{S\mathcal{E}}$ has been implemented in [6]. The total qubit-environment Hamiltonian is given by

$$\hat{H} = \hat{H}_\mathcal{E} + \hat{H}_{S\mathcal{E}}.$$

The driving is a result of a slow $-\tau_Q \gg 1$ - ramp down of a magnetic field

$$g(t) = 1 - t/\tau_Q, \quad (5)$$

which is equivalent to (1) taken with $g_c = 1$. Evolution starts at $t = -\infty$ with the qubit in a pure state superposition of $c_+ |\uparrow\rangle + c_- |\downarrow\rangle$ and the environment in

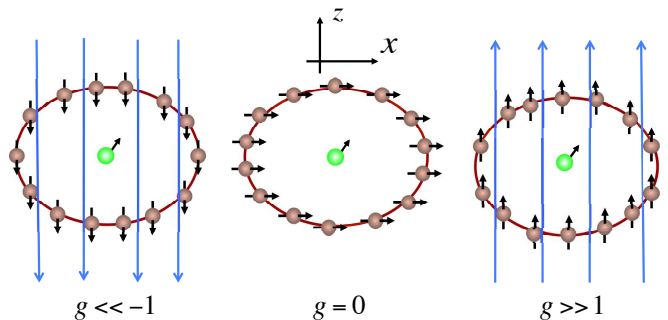


FIG. 1: (color online). The central spin-1/2 (qubit) interacts with the Ising spin environment whose quantum phase transition is driven by an external magnetic field. For large initial and final fields – right and left panel, respectively – the environment is in the paramagnetic phase: its spins align with the field. For small fields ($|g(t)| < 1$, center panel) Ising chain enters a ferromagnetic phase, where its spins try to align with x or $-x$ breaking the symmetry of the Ising Hamiltonian.

its instantaneous ground state $|GS(t = -\infty)\rangle$. The composite wave function $|\psi\rangle$ of the system is given initially by

$$|\psi(t = -\infty)\rangle = (c_+ |\uparrow\rangle + c_- |\downarrow\rangle) \otimes |GS(t = -\infty)\rangle.$$

A straightforward calculation then shows that

$$\begin{aligned} |\psi(t)\rangle &= \hat{T} e^{-i \int_{-\infty}^t dt \hat{H}(g(t))} |\psi(t = -\infty)\rangle \\ &= c_+ |\uparrow\rangle \otimes \hat{T} e^{-i \int_{-\infty}^t dt \hat{H}_\mathcal{E}(g(t) + \delta)} |GS(t = -\infty)\rangle \\ &\quad + c_- |\downarrow\rangle \otimes \hat{T} e^{-i \int_{-\infty}^t dt \hat{H}_\mathcal{E}(g(t) - \delta)} |GS(t = -\infty)\rangle \\ &= c_+ |\uparrow\rangle \otimes |\varphi_+(t)\rangle + c_- |\downarrow\rangle \otimes |\varphi_-(t)\rangle, \end{aligned}$$

where \hat{T} is the time-ordering operator, and evolution of the environmental states coupled to up-down qubit states is given by

$$i \frac{\partial}{\partial t} |\varphi_\pm(t)\rangle = \hat{H}_\mathcal{E}(g(t) \pm \delta) |\varphi_\pm(t)\rangle. \quad (6)$$

Therefore, evolution of the system depends on the dynamics of two Ising branches evolving in an effective magnetic field given by $g(t) \pm \delta$.

The reduced density matrix of the qubit in the $\{|\uparrow\rangle, |\downarrow\rangle\}$ basis reads

$$\rho_S(t) = \text{Tr}_\mathcal{E} |\psi(t)\rangle \langle \psi(t)| = \begin{pmatrix} |c_+|^2 & c_+ c_-^* d^*(t) \\ c_+^* c_- d(t) & |c_-|^2 \end{pmatrix},$$

where $d(t) = \langle \varphi_+(t) | \varphi_-(t) \rangle$ is the decoherence factor. We study its squared modulus,

$$D = |d(t)|^2 = |\langle \varphi_+(t) | \varphi_-(t) \rangle|^2,$$

also known as the decoherence factor; we follow this nomenclature below. When $D = 1$, the qubit is in a pure state, but when $D = 0$ it is completely decohered.

IV. EXACT SOLUTION

Dynamics of the decoherence factor can be obtained analytically by solving (6). This can be done after mapping the spins onto non-interacting fermions via the Jordan-Wigner transformation [14]. We introduce after Dziarmaga the Bogolubov modes u_k^\pm and v_k^\pm through

$$|\varphi_\pm(t)\rangle = \prod_{k>0} [u_k^\pm(t)|0_k, 0_{-k}\rangle - v_k^\pm(t)|1_k, 1_{-k}\rangle], \quad (7)$$

where $|m_k, m_{-k}\rangle$ describes the state with $m = 0, 1$ pairs of quasiparticles with momentum $k = (2s + 1)\pi/N$, $s = 0, 1, \dots, N/2 - 1$. We consider even N . In this formalism one easily finds that

$$D(t) = \prod_{k>0} F_k(t), \quad F_k(t) = |u_k^{+\ast}(t)u_k^-(t) + v_k^{+\ast}(t)v_k^-(t)|^2. \quad (8)$$

We will refer to F_k to describe dynamics of decoherence from the momentum space angle. We call it a decoherence factor in momentum space. Using (8) we find that for thermodynamically large environments

$$D(t) \approx \exp\left(-\frac{N}{2\pi} \int_0^\pi dk \ln F_k^{-1}(t)\right). \quad (9)$$

The above integral representation shall be accurate for time instants t for which $\ln F_k(t)$ is non-singular $\forall k$ [29]. All we need now are the Bogolubov modes at various stages of evolution. The modes evolve according to [14]

$$\begin{aligned} i \frac{d}{dt} v_k^\pm &= -2(g(t) \pm \delta - \cos k)v_k^\pm + 2 \sin k u_k^\pm, \\ i \frac{d}{dt} u_k^\pm &= 2(g(t) \pm \delta - \cos k)u_k^\pm + 2 \sin k v_k^\pm. \end{aligned}$$

We apply the transformation $t'_\pm = 4\tau_Q \sin k (-g(t) \mp \delta + \cos k)$. Defining $\tau'_Q = 4\tau_Q \sin^2 k$ we end up with the Landau-Zener system,

$$i \frac{d}{dt'_\pm} \begin{pmatrix} v_k^\pm \\ u_k^\pm \end{pmatrix} = \frac{1}{2} \begin{pmatrix} \frac{t'_\pm}{\tau'_Q} & 1 \\ 1 & -\frac{t'_\pm}{\tau'_Q} \end{pmatrix} \begin{pmatrix} v_k^\pm \\ u_k^\pm \end{pmatrix}, \quad (10)$$

that can be solved with the Weber functions (see e.g. [30]). The initial conditions are $v_k^\pm(t'_\pm = -\infty) = 0$ and $u_k^\pm(t'_\pm = -\infty) = 1$. To express the solution in a compact form we introduce: $z_\pm = t'_\pm \exp(i\pi/4)/\sqrt{\tau'_Q}$ and $n = -i\tau'_Q/4$. The exact solution reads

$$v_k^\pm(t) = \frac{\sqrt{\tau'_Q}}{2} \exp(-\pi\tau'_Q/16) \mathcal{D}_{-n-1}(iz_\pm) \quad (11)$$

$$u_k^\pm(t) = \exp(-\pi\tau'_Q/16) \exp(i\pi/4) \times \\ [(1+n)\mathcal{D}_{-n-2}(iz_\pm) + iz_\pm \mathcal{D}_{-n-1}(iz_\pm)] \quad (12)$$

where $\mathcal{D}_m(iz)$ is the Weber function [31]. It is simplified in the Appendix.

V. DYNAMICS OF DECOHERENCE

The quench starts with the environment in the paramagnetic phase ($g(t) > 1$), moves the environment across the ferromagnetic phase ($-1 < g(t) < 1$), and finally brings it to the “other” paramagnetic phase ($g(t) < -1$). The critical points are located at $g_c = \pm 1$. Substituting $z, \nu = 1$ into (2) and (3) results in $\hat{g} \sim 1/\sqrt{\pi Q}$ and $\hat{\xi} \sim \sqrt{\pi Q}$ [12]. The non-equilibrium length scale $\hat{\xi}$ provides the typical spacing of kinks (spin flips) excited during the transition [12, 14]. Dynamics of the decoherence factor is depicted in Figs. 2-4.

As the field polarizing spins in the chain is ramped down (5), environment’s sensitivity to external influence increases. This results in enhanced decoherence visible as a gradual decrease of the decoherence factor D away from the critical point (Fig. 2). Initially evolution proceeds adiabatically and D is identical to ground state fidelity of the environment [17, 18, 20]. Namely, to the squared overlap between the ground states of $\hat{H}_E(g \pm \delta)$: $|\langle GS(g + \delta) | GS(g - \delta) \rangle|^2$. As is derived in the Appendix, away from the critical points, $|g(t) - g_c| \gg \delta$, we have for the k modes evolving adiabatically

$$F_k(t) = 1 - \frac{\delta^2 \sin^2 k}{(1 - 2g(t) \cos k + g(t)^2)^2} + \mathcal{O}(\delta^4), \quad (13)$$

which compares well to numerics (Fig. 5a; see also Figs. 5c and 5e). Using (9) we obtain in the paramagnetic phase that

$$D(t) \approx \exp\left(-\frac{N\delta^2}{4g(t)^2(g(t)^2 - 1)}\right). \quad (14)$$

Just above the first critical point, $1 < g < 1 + \hat{g}$, the adiabatic approximation breaks down and decoherence speeds up; decoherence factor decreases substantially. This happens because (i) environment’s sensitivity is enhanced by quantum criticality amplifying the perturbation resulting from the coupling to the qubit system; (ii) the environment is no longer in the ground state: quench is taking it into a superposition of energy eigenstates.

As the environment is driven past the first critical point at $g_c = 1$, there are either partial revivals (Figs. 2 and 3) or a monotonic decay (Fig. 4) of coherence between the critical points. They result from non-equilibrium dynamics around the critical point leading to excitation of small k modes (the gap in the excitation spectrum closes for $k = 0$ at $g_c = 1$). Expanding (11) and (12) – see the Appendix – we find a remarkably simple and accurate solution for the problem. For low k modes, i.e., $k \sim \hat{k} = \mathcal{O}(1)/\sqrt{\pi Q}$ (4), we get

$$F_k(t) = 1 - 4 \left(e^{-2\pi\tau_Q k^2} - e^{-4\pi\tau_Q k^2} \right) \sin^2 \phi(t), \quad (15)$$

where $\phi(t) \approx 4(1 - g(t))\tau_Q \delta = 4t\delta$. As shown in Fig. 5b – see also Fig. 5d – there is a very good agreement between (15) and numerics. The larger k modes, those

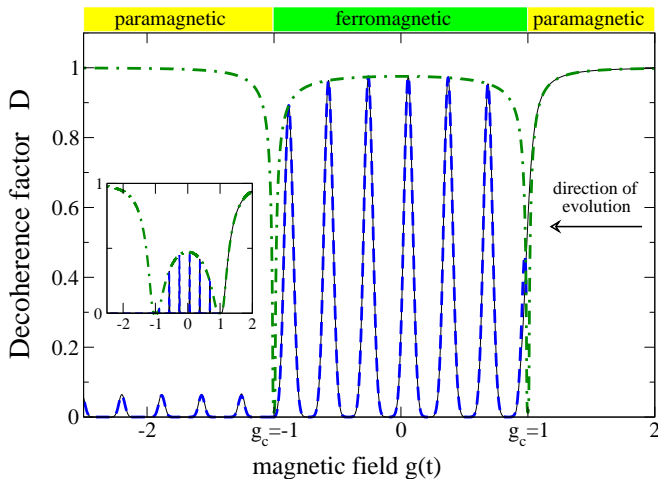


FIG. 2: (color online) Decoherence during a quench: a quasi-periodic regime between the critical points. Black solid line shows the result obtained from numerical integration of (10). Our analytical approximations are superimposed on it as a blue dashed line: (16) for $g(t) \in (-1, 1)$ and (19) for $g(t) < -1$. The green dashed-dotted line is the adiabatic result equivalent to ground state fidelity ($\tau_Q \rightarrow \infty$ limit): (A1) combined with (8). Numerical solution almost perfectly overlaps with analytical results away from the critical points: $|g(t) - g_c| > \hat{g}, \delta$. The main plot shows that for moderate environment sizes – $N = 1000$ here – almost perfect revivals of coherence take place between the critical points, but coherence is virtually lost after driving the environment through the second critical point. The inset shows the same, but for $N = 30,000$. It illustrates that for very large environments there is little coherence left after passing the first critical point and the qubit is completely decohered after crossing the second critical point. Note that ground state fidelity provides the envelope for the revivals of coherence between the critical points. We used here $\delta = 10^{-2}$ and $\tau_Q = 250$.

for which $k \gg \hat{k}$, evolve adiabatically through the critical point. Their decoherence factor F_k reads (13), which is illustrated in Fig. 5c, where again numerics matches well our theory.

One striking feature of (15) is that there is a characteristic momentum scale imprinted by the quench. It is predicted by the KZ theory (4). Indeed, (15) depends on momentum through the combination of k/\hat{k} . Moreover, the modes centered around

$$k_m = \sqrt{\frac{\ln 2}{2\pi}} \frac{1}{\sqrt{\tau_Q}}$$

contribute most to non-equilibrium decoherence resulting from crossing the first critical point: (15) has a single minimum at k_m . Interestingly, the position of this minimum is fixed in the post-transition state, $dk_m/dt = 0$ for $g(t) < 1$. It means that the characteristic length scale imprinted by the non-equilibrium critical dynamics remains “frozen” after the critical point was passed. This is in perfect agreement with the adiabatic-impulse picture of dynamics proposed by the quantum KZ theory

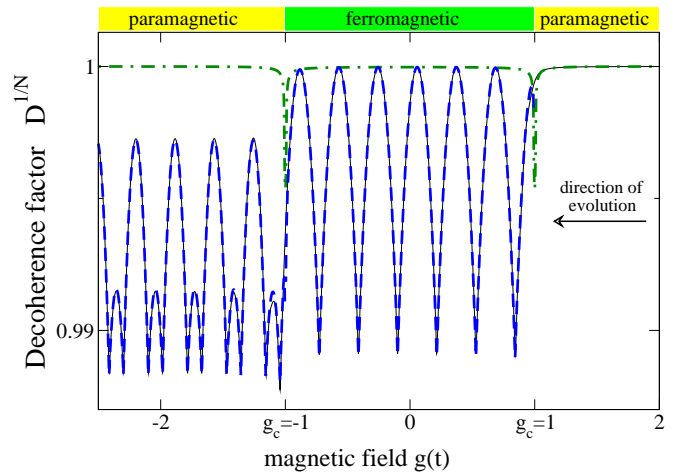


FIG. 3: (color online) Same as in Fig. 2, except we consider here N -th root of the decoherence factor D illustrating details of dynamics of decoherence in the large N limit. Numerical result (black line) is obtained by calculating $D^{1/N}$ for $N = 2000$ environmental spins. N -th root of ground state fidelity (green dashed-dotted line) is calculated for the same N .

[11, 12].

Combining (13), (15), and (9) we get

$$D(t) \approx \exp\left(-\frac{N\delta^2}{4(1-g(t)^2)}\right) \exp\left(-\frac{N}{2\pi} \frac{f[\phi(t)]}{\sqrt{\tau_Q}}\right), \quad (16)$$

where $f[\phi] = -\frac{1}{\sqrt{2\pi}} \int_0^\infty ds \ln[1 - 4(e^{-s^2} - e^{-2s^2}) \sin^2 \phi]$ and $\phi \approx 4t\delta$ (the $\tau_Q \rightarrow \infty$ limit was assumed to simplify the upper integration limit in $f[\phi]$) [29]. The first factor above is again ground state fidelity, but this time in the ferromagnetic phase: notice the lack of g^{-2} factor as compared to the paramagnetic phase result (14). The second one comes from non-equilibrium environment excitation happening around the first critical point. Indeed, since we already know that the quench enforces $F_k = F(k/\hat{k})$ for low momentum modes, a simple change of the integration variable to k/\hat{k} in (9) gives the $\tau_Q^{-\nu/(1+z\nu)} = \tau_Q^{-1/2}$ factor in (16); see also Sec. VI. Thus, we show analytically that for the Ising chain non-equilibrium contribution to the decoherence rate encodes *universal* information about the criticality of the environment via the z and ν exponents. This information is recorded in the decohering state of the simplest quantum system, the spin-1/2 qubit, and should be experimentally accessible.

The non-universal contribution to non-equilibrium decoherence, $f[\phi(t)]$ from (16), leads to rich dynamics of decoherence. We observe partial revivals of coherence between the critical points taking place when the environment-qubit coupling is strong enough: $\delta > \pi/16\tau_Q$. They happen in the magnetic field (g) domain with the period of $\pi/4\tau_Q\delta$. The envelope of these revivals is given accurately by ground state fidelity: at the peaks of the decoherence factor non-adiabatic F_k 's (15) equal unity and so only adiabatic modes contribute to

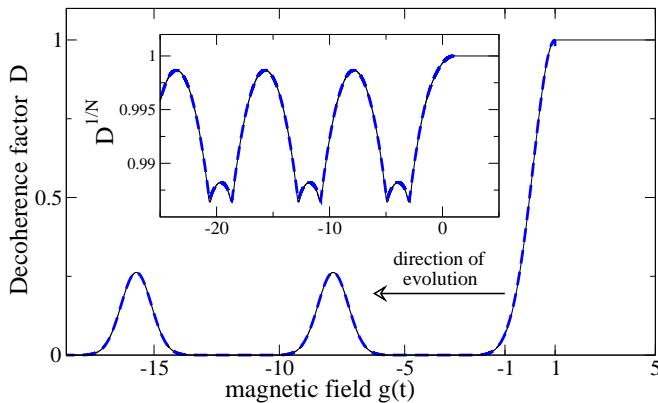


FIG. 4: (color online) Decoherence during a quench: a gaussian regime between the critical points. Solid black line shows the result coming from numerical integration of (10). The dashed blue line shows our analytical approximations: the gaussian result (17) between the critical points [$g(t) \in (-1, 1)$] and (19) past the second critical point [$g(t) < -1$]. The inset shows N -th root of the data from the main plot: it illustrates details of the revivals of coherence past the second critical point. The parameters for this plot are: $N = 1000$, $\delta = 4 \times 10^{-4}$, and $\tau_Q = 250$. Except for δ , they are the same as in Fig. 2. The switch from coherence revivals (Fig. 2) to monotonic decay of coherence between the critical points is a result of lowering the qubit – environment coupling δ below the $\pi/16\tau_Q$ threshold.

the decoherence factor there. As ground state fidelity is smaller than unity, the revivals of coherence cannot be perfect (Fig. 2). The presence of the adiabatic “fidelity” envelope, however, may allow for *measurement* of ground state fidelity at the peaks of the decoherence factor: an interesting observation as we have here an out of equilibrium system and ground state fidelity is an equilibrium quantity.

In the opposite limit of weak coupling between the environment and the qubit, $\delta < \pi/16\tau_Q$, decoherence factor decreases monotonically till the second critical point at $g_c = -1$. In particular, when $\delta \ll \pi/16\tau_Q$ expansion of (16) gives gaussian decay of D (Fig. 4):

$$D(t) \approx \exp\left(\frac{-N8\delta^2 t^2 (\sqrt{2}-1)}{\pi\sqrt{\tau_Q}}\right) \exp\left(\frac{-N\delta^2}{4(1-g(t)^2)}\right). \quad (17)$$

Even richer dynamics of decoherence emerges when the magnetic field reverses polarity and drives the system past the second critical point at $g_c = -1$ (Figs. 2-4). Indeed, at the second critical point the modes $k \sim \pi - \hat{k}$ become excited because the gap closes there at $k = \pi$. This means that the decoherence factor F_k will be given by (15) for $k \sim \hat{k}$, (13) for $\hat{k} \lesssim k \lesssim \pi - \hat{k}$, and

$$F_k(t) = 1 - 4 \left(e^{-2\pi\tau_Q(k-\pi)^2} - e^{-4\pi\tau_Q(k-\pi)^2} \right) \sin^2 \eta(t), \quad (18)$$

for $k \sim \pi - \hat{k}$, where $\eta(t) \approx 4(g(t)+1)\tau_Q\delta$ (see the Appendix). This is illustrated in Figs. 5d-f, where good

agreement between theory and numerics is confirmed. Similarly as above, the momentum scale from the KZ theory leaves a long lasting imprint here: the modes most contributing to non-equilibrium decoherence due to crossing of the second critical point are centered around $k = \pi - k_m$ for $g(t) < -1$: (18) has a minimum at such k .

Marrying (13), (15) and (18) with (9) we obtain [29]

$$D(t) \approx \exp\left(-\frac{N\delta^2}{4g(t)^2(g(t)^2-1)}\right) \times \exp\left(-\frac{N}{2\pi} \frac{f[\phi(t)] + f[\eta(t)]}{\sqrt{\tau_Q}}\right). \quad (19)$$

Comparing (19) to (16) we see one additional factor, $\exp(-Nf[\eta(t)]/2\pi\sqrt{\tau_Q})$, due to non-equilibrium transition across the second critical point. We would like to stress again that dynamics across the two critical points happens “independently” because the gap of the environment closes at $g_c = 1$ ($g_c = -1$) for $k_0 = 0$ ($k_0 = \pi$): the first (second) transition excites small (large) momentum modes. Excitations created around the two critical points impose the same revival period for D , but their phases are shifted. It leads to destructive interference damping the amplitude of the partial revivals dramatically. We also note again that (13-19) are derived away from the critical points, i.e., for $|g(t) - g_c| \gg \delta, \hat{g}$.

Finally, we compare the quench-amplified decoherence factor to the one resulting from the adiabatic quench ($\tau_Q = \infty$). We see in Figs. 2 and 3 that decoherence can be much stronger in the driven environment: compare the green dashed-dotted line to the blue dashed line. This is related to the excitations (kinks for the Ising chain [12, 14]) appearing in a non-adiabatic quench. Thus, susceptibility of many-body environments to perturbations reflects not just their instantaneous Hamiltonians or eigenstates, but also their actual (non-equilibrium) state encoding the quench history.

VI. GENERAL SCALING RESULT

A variety of systems have the decoherence factor D given in the product form (8). This factorization appears when a many-body environment is described by a product wave function in momentum space such as (7). This is the case for some quantum magnets (XY, Ising, Kitaev, etc.) [15], conventional superconductors (either electronic [32] or those emulated by cold atoms [33]), and liquid ^3He [34]. As for the Ising case, excitation of these environments during a dynamical phase transition shall imprint a non-equilibrium length scale $\hat{\xi}$ and momentum scale \hat{k} , (3) and (4), respectively. Note that we again assume that the external field driving the QPT is quenched according to (1). It is thus natural to assume that for those systems as well overlap F_k between dynamically excited states of the environment depends on momentum through $(k - k_0)/\hat{k}$ combination: $F_k = F((k - k_0)/\hat{k})$,

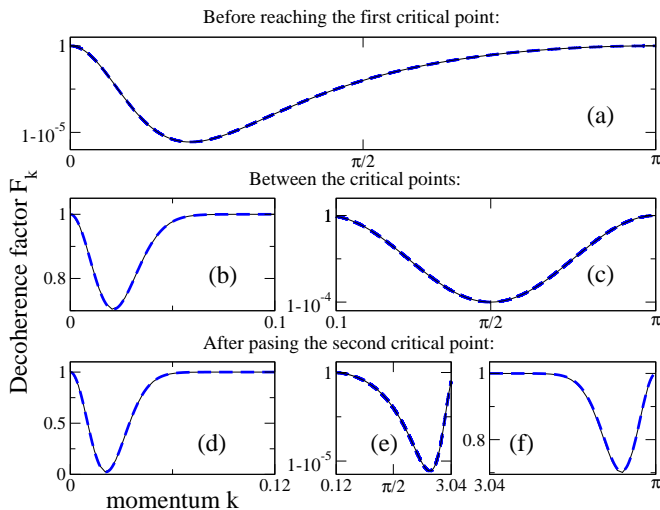


FIG. 5: (color online) Decoherence factor F_k during the quench. Solid black lines show numerics based on (10). The blue dashed lines illustrate our analytical approximations. Before reaching the critical point at $g_c = 1$ modes evolve adiabatically: panel (a) made for $g(t) = 2$. The adiabatic result (13) fits numerics for all momenta. Between the critical points – panels (b) and (c) made for $g(t) = 0$ – low k modes are excited due to driving across $g_c = 1$, while the large k modes evolve adiabatically. The former is illustrated in panel (b) where (15) fits numerics, while the latter is depicted in panel (c) where (13) matches numerics. Panels (d-f) prepared for $g(t) = -2$ show what happens after passing the second critical point at $g_c = -1$: low k modes are still excited due to driving across $g_c = 1$, intermediate modes evolve adiabatically, while large k modes are excited by crossing the $g_c = -1$ critical point. This is theoretically described by (15), (13) and (18) depicted in panels (d), (e) and (f), respectively. Note that despite the tiny range of variation of the adiabatically evolving modes – panels (a), (c) and (e) – the striking envelope of the quasi-periodic revivals of coherence between the critical points comes from these modes. Solid black lines (numerics) have been obtained for $N = 2000$, $\tau_Q = 250$ and $\delta = 10^{-2}$. The same τ_Q and δ have been used to get the dashed lines (analytical approximations).

where k_0 is the momentum for which the gap closes. When that happens, exchanging the product (8) into an integral similarly as in (9), one can easily derive that contribution to the decoherence factor coming from low energy modes excited by the quench is given by

$$\hat{D}(t) \approx \exp\left(-N\Upsilon(t)/\tau_Q^{r\nu/(1+z\nu)}\right). \quad (20)$$

Above $\tau_Q^{r\nu/(1+z\nu)}$ captures the universality-class dependence of decoherence caused by non-equilibrium crossing of the quantum critical point, while $\Upsilon(t)$ stands for the non-universal (system-dependent) response to driving. Moreover, r is the environment dimensionality and N is the environment size (number of spins/particles/etc.). Note also that the contribution of the momentum modes that were not excited by the quench adds another factor besides \hat{D} to the full decoherence factor D in complete

analogy to what we have seen for the Ising environment in Eqs. (16) and (19). We expect that this “adiabatic” factor is well approximated by instantaneous ground state fidelity as was shown to be the case in the Ising model.

Finally, we mention that (20) reveals also that non-equilibrium decoherence is expected to be exponential in the number of topological defects created by the quench:

$$N/\hat{\xi}^r \sim N/\tau_Q^{r\nu/(1+z\nu)}.$$

Note that $\hat{\xi}$ provides a typical distance between topological defects created by the quench.

VII. CONCLUSIONS

We have demonstrated rich manifestations of decoherence induced by a dynamical phase transition in the environment. In particular, we have shown that near the critical point decoherence is dramatically enhanced not just by the increased susceptibility, but also by the excitations that depend on the past history of the system. Our results provide a strong indication of a universality-class dependent behavior that bears remarkable similarity to the dynamics of defect formation in non-equilibrium phase transitions [24, 25].

This work should stimulate future theoretical studies. In particular, it would be interesting to study both universal and system-dependent contributions to decoherence dynamics in other out-of-equilibrium environments, especially those described by a different universality class than the Ising model. It would be also interesting to find out if a similar description can be worked out for systems whose wave function is not given by the product over momentum modes. Generalization of our results to finite temperatures can provide yet another extension of our work.

We expect that our findings will be experimentally accessible in future cold atom/ion quantum simulators of condensed matter systems [35]. Moreover, it should be also possible to extend them to optomechanical systems where a cold atom cloud undergoing a QPT (the environment) is coupled to a mirror (a quantum system) [36]. Finally, generalizing the idea from [8], the non-equilibrium enhancement of the decoherence rate of the qubit might find its applications in magnetometry.

VIII. ACKNOWLEDGEMENTS

This work is supported by U.S. Department of Energy through the LANL/LDRD Program. We acknowledge stimulating discussions with Rishi Sharma, and thank Jacek Dziarmaga for his comments on the manuscript.

Appendix : Simplification of the exact solution

Exact solutions (11) and (12) for the Bogolubov modes can be simplified for (i) modes evolving adiabatically; (ii) small momentum modes excited by crossing the critical point at $g_c = 1$; and (iii) for large momentum modes excited due to non-adiabatic crossing of the critical point at $g_c = -1$. The resulting expressions can be used to simplify decoherence factor in momentum space: F_k . Their knowledge allows for accurate determination of the decoherence factor D away from the critical points. We will briefly outline below how compact expressions for F_k can be derived.

Adiabatic evolution of modes: Modes evolving adiabatically are described by well-known ground state solutions taken at *instantaneous* value of the magnetic field $g(t)$ [14, 26]. This implies that

$$v_k^\pm = \cos(\theta^\pm/2), \quad u_k^\pm = \sin(\theta^\pm/2),$$

where $\theta^\pm \in [0, \pi]$, $\cos(\theta^\pm) = \epsilon_\pm / \sqrt{1 + \epsilon_\pm^2}$, and $\epsilon_\pm = (-g(t) \mp \delta + \cos k) / \sin k$. The decoherence factor in momentum space takes the compact form

$$F_k = \cos^2 \left(\frac{\theta^+ + \theta^-}{2} \right), \quad (\text{A1})$$

which can be simplified by the Taylor expansion

$$F_k = 1 - \frac{\delta^2 \sin^2 k}{(1 - 2g \cos k + g^2)^2} + \mathcal{O}(\delta^4).$$

Small momentum expansion for the modes excited after crossing the critical point at $g_c = 1$: We assume here that $g(t) < 1$ and consider only $k \ll \pi/4$ relevant for slow transitions ($\tau_Q \gg 1$). Our expansion of (11) and (12) is based on large $|iz_\pm|$ expansion of the Weber functions. We define $z_\pm = \alpha_\pm \exp(i\pi/4)$, where

$$\alpha_\pm(t) = 2\sqrt{\tau_Q}(-g(t) \mp \delta + \cos k).$$

To expand Weber functions we assume below that $\alpha_\pm \gg 1$, which implies that

$$\tau_Q \gg \frac{1}{4(1 - g(t) - \delta)^2}$$

for small k modes. This condition can be equivalently rewritten to

$$1 - g(t) \gg \delta, \mathcal{O}(1)/\sqrt{\tau_Q}.$$

To proceed, we need the following identities [31]. For $|\arg(s)| < 3\pi/4$

$$\mathcal{D}_m(s) = e^{-s^2/4} s^m [1 + \mathcal{O}(s^{-2})],$$

while for $\pi/4 < \arg(s) < 5\pi/4$

$$\mathcal{D}_m(s) = e^{im\pi} \mathcal{D}_m(-s) + \frac{\sqrt{2\pi}}{\Gamma(-m)} e^{i(m+1)\pi/2} \mathcal{D}_{-m-1}(-is).$$

Keeping only the leading terms in the expansion of the Weber functions in (11) and (12), we find that

$$v_k^\pm(t) \approx \sqrt{\frac{\pi\tau_Q'}{2}} \frac{e^{-\pi\tau_Q'/8} e^{-i[\alpha_\pm^2(t) + \tau_Q' \ln \alpha_\pm(t)]/4}}{\Gamma(1 - i\tau_Q'/4)}, \quad (\text{A2})$$

$$u_k^\pm(t) \approx e^{-\pi\tau_Q'/4} e^{i\pi/4} e^{i[\alpha_\pm^2(t) + \tau_Q' \ln \alpha_\pm(t)]/4}. \quad (\text{A3})$$

Having these expressions we get

$$v_k^{+*}(t)v_k^-(t) = [1 - \exp(-\pi\tau_Q'/2)] \exp(-i\chi(t)), \quad (\text{A4})$$

$$u_k^{+*}(t)u_k^-(t) = \exp(-\pi\tau_Q'/2) \exp(i\chi(t)), \quad (\text{A5})$$

where

$$\chi(t) = [\alpha_-^2(t) - \alpha_+^2(t)]/4 + \tau_Q' \ln[\alpha_-(t)/\alpha_+(t)]/4. \quad (\text{A6})$$

Next we additionally simplify these results by considering $k \ll \pi/4$ and $\delta \ll 1$ limits. These assumptions result in $\tau_Q' \approx 4k^2\tau_Q$ and $\chi(t) \approx 4\delta\tau_Q[1 - g(t)]$. Substituting $g(t) = 1 - t/\tau_Q$ into (A6) one gets $\chi(t) \approx 4t\delta$. After some algebra these expressions allow for writing the decoherence factor in momentum space as

$$F_k(t) \approx 1 - 4 \sin^2(4t\delta) \left(e^{-2\pi\tau_Q k^2} - e^{-4\pi\tau_Q k^2} \right). \quad (\text{A7})$$

Large momentum expansion for the modes excited after crossing the critical point at $g_c = -1$: We assume here that $g(t) < -1$. The calculations are similar as above with the only difference that slow driving through the critical point at $g_c = -1$ excites momentum modes near $k = \pi$ rather than those close to $k = 0$. The small k modes, excited during crossing the critical point at $g_c = 1$, are not affected by driving through the critical point at $g_c = -1$: (A2) - (A7) hold for $g(t) < -1$. The solutions (A2) and (A3) are valid again, but the expansion now requires

$$\tau_Q \gg \frac{1}{4(-1 - g(t) - \delta)^2},$$

because we need to substitute $\cos k \approx -1$ into α_\pm . Equations (A4) and (A5) are the same, but the phase χ and modified quench time scale τ_Q' have different expansions for $\delta \ll 1$ and $\pi - k \ll \pi/4$: $\chi(t) \approx -4\tau_Q\delta(1 + g)$ and $\tau_Q' \approx 4(k - \pi)^2\tau_Q$.

Wrapping it up we obtain

$$F_k(t) \approx 1 - 4 \left(e^{-2\pi\tau_Q(k-\pi)^2} - e^{-4\pi\tau_Q(k-\pi)^2} \right) \sin^2 \eta(t),$$

where $\eta(t) = 4\tau_Q\delta(1 + g(t))$.

-
- [1] W. H. Zurek, *Rev. Mod. Phys.* **75**, 715 (2003).
- [2] M. Schlosshauer, *Decoherence and the Quantum-to-Classical Transition* (Springer Verlag, 2007).
- [3] W. H. Zurek, *Phys. Rev. D* **24**, 1516 (1981); F. M. Cucchietti, J. P. Paz, and W. H. Zurek, *Phys. Rev. A* **72**, 052113 (2005).
- [4] R. Hanson, V. V. Dobrovitski, A. E. Feiguin, O. Gywat, and D. D. Awschalom, *Science* **320**, 352 (2008).
- [5] H. Bluhm *et al.*, *Nature Phys.* **7**, 109 (2011); L. Cywiński, *Acta Phys. Pol. A* **119**, 576 (2011).
- [6] J. Zhang, X. Peng, N. Rajendran, and D. Suter, *Phys. Rev. Lett.* **100**, 100501 (2008).
- [7] W. H. Zurek, F. M. Cucchietti, and J.P. Paz, *Acta Phys. Pol. B* **38**, 1685 (2007).
- [8] G. Goldstein *et al.*, *Phys. Rev. Lett.* **106**, 140502 (2011).
- [9] H. T. Quan, Z. Song, X. F. Liu, P. Zanardi, and C. P. Sun, *Phys. Rev. Lett.* **96**, 140604 (2006).
- [10] C. Cormick and J. Pablo Paz, *Phys. Rev. A* **77**, 022317 (2008).
- [11] B. Damski, *Phys. Rev. Lett.* **95**, 035701 (2005).
- [12] W. H. Zurek, U. Dorner, and P. Zoller, *Phys. Rev. Lett.* **95**, 105701 (2005).
- [13] A. Polkovnikov, *Phys. Rev. B* **72**, 161201 (2005).
- [14] J. Dziarmaga, *Phys. Rev. Lett.* **95**, 245701 (2005).
- [15] J. Dziarmaga, *Adv. Phys.* **59**, 1063 (2010).
- [16] L. E. Sadler, J. M. Higbie, S. R. Leslie, M. Vengalattore and D. M. Stamper-Kurn, *Nature* **443**, 312 (2006).
- [17] P. Zanardi and N. Paunković, *Phys. Rev. E* **74**, 031123 (2006).
- [18] S.-J. Gu, *Int. J. Mod. Phys. B* **24**, 4371 (2010).
- [19] A. Osterloh, L. Amico, G. Falci, and R. Fazio, *Nature (London)* **416**, 608 (2002).
- [20] M. M. Rams and B. Damski, *Phys. Rev. Lett.* **106**, 055701 (2011).
- [21] S. Mostame, G. Schaller, and R. Schützhold, *Phys. Rev. A* **76**, 030304 (2007).
- [22] D. Patanè, A. Silva, L. Amico, R. Fazio, and G. E. Santoro, *Phys. Rev. Lett.* **101**, 175701 (2008).
- [23] L. Cincio, J. Dziarmaga, J. Meisner, and M. M. Rams, *Phys. Rev. B* **79**, 094421 (2009).
- [24] T.W.B. Kibble, *J. Phys. A* **9**, 1387 (1976); *Phys. Rep.* **67**, 183 (1980); T.W.B. Kibble, *Physics Today* **60**, 47 (2007).
- [25] W.H. Zurek, *Nature (London)* **317**, 505 (1985); *Acta Phys. Pol. B* **24**, 1301 (1993); *Phys. Rep.* **276**, 177 (1996).
- [26] S. Sachdev, *Quantum Phase Transitions* (Cambridge University Press, Cambridge, U.K., 1999).
- [27] R. Coldea *et al.*, *Science* **327**, 177 (2010).
- [28] J. Zhang *et al.*, *Phys. Rev. A* **79**, 012305 (2009).
- [29] Note that replacement of the product over k modes (8) by the integral (9) is questionable when for some k we have $F_k = 0$. In particular, if it happens for $k \neq 0$ the decoherence factor D will depend on the exact value of the discrete momenta contributing to the product (8) because in such a case a single k mode may set (8) to zero. For the Ising environment that we study discretization in momentum space is fixed by the environment size N and is overlooked by the $N \rightarrow \infty$ limit assumed in (9). This implies that our analytical approximations (15) and (18) shall not be used to obtain (16) and (19) at time instants t for which $F_k(t) = 0$ for some k . This happens in (15) when $\sin^2 \phi(t) = 1$ and in (18) when $\sin^2 \eta(t) = 1$. Analogical problems with exchange of the product by an integral are described in detail in the context of ground state fidelity of the XY model in M. M. Rams and B. Damski e-print arXiv:1104.4104 (2011).
- [30] B. Damski and W. H. Zurek, *Phys. Rev. A* **73**, 063405 (2006).
- [31] E. T. Whittaker and G. N. Watson, *A Course of Modern Analysis* (Cambridge University Press, Cambridge, England, 1958).
- [32] M. Tinkham, *Introduction to superconductivity* (McGraw-Hill, New York, 1996).
- [33] W. Ketterle and M.W. Zwierlein, *Riv. Nuovo Cimento* **31**, 247 (2008).
- [34] D. Vollhardt and P. Wölfle, *The superfluid phases of Helium 3* (Taylor and Francis, 1990).
- [35] M. Lewenstein, A. Sanpera, V. Ahufinger, B. Damski, A. Sen(De), and U. Sen, *Adv. Phys.* **56**, 243 (2007).
- [36] J. P. Santos, F. L. Semião, and K. Furuya, *Phys. Rev. A* **82**, 063801 (2010).